polysaccharides

MDPI

Article

Study of the Structure–Property Relationships of Starch from Andean Varieties of *Ullucus tuberosus*

David Choque-Quispe [1,*], Elias Saúl Ortega Pacheco [1,*], Jorge W. Elias-Silupu [2], Yakov Felipe Carhuarupay-Molleda [3], Miriam Calla-Florez [4], Antonieta Mojo-Quisani [4], Lourdes M. Zamalloa-Puma [4], Lucero Quispe Chambilla [5], Hilka Mariela Carrión Sánchez [5], Edward Arostegui León [6], Carlos Alberto Benites Castañeda [7] and Juan Quispe Ccama [8]

1 Agroindustrial Engineering Academic Department, José María Arguedas National University, Andahuaylas 03701, Peru
2 Science and Engineering Academic Department, Ciro Alegria National University, Huamachuco 13301, Peru; jelias@unca.edu.pe
3 Basic Sciences Department, José María Arguedas National University, Andahuaylas 03701, Peru; ycarhuarupay@unajma.edu.pe
4 Agroindustrial Engineering Academic Department, Universidad Nacional de San Antonio Abad del Cusco, Cusco 08000, Peru; miriam.calla@unsaac.edu.pe (M.C.-F.); antonieta.mojo@unsaac.edu.pe (A.M.-Q.); lourdes.zamalloa@unsaac.edu.pe (L.M.Z.-P.)
5 Food Engineering Academic Department, Intercultural de Quillabamba National University, Quillabamba 08741, Peru; lucero.quispe@uniq.edu.pe (L.Q.C.); hilka.carrion@uniq.edu.pe (H.M.C.S.)
6 Environmental Engineering Academic Department, José María Arguedas National University, Andahuaylas 03701, Peru; earostegui@unajma.edu.pe
7 Agricultural and Forestry Engineering Department, Ciro Alegria National University, Huamachuco 13301, Peru; cbenites@unca.edu.pe
8 Agroindustrial Engineering Academic Department, Universidad Nacional del Altiplano, Puno 21001, Peru; jquispecc@unap.edu.pe
* Correspondence: dchoque@unajma.edu.pe (D.C.-Q.); es.ortega33@gmail.com (E.S.O.P.)

Abstract

Various tubers are cultivated in the Peruvian Andes. Olluco (*Ullucus tuberosus*) is consumed locally for its culinary qualities and nutritional value. In addition to its resistance to pests and extreme climatic conditions, this Andean tuber is an important source of starch. In this study, the extraction and characterization of the physical, chemical, technofunctional, and thermal properties of olluco starches from the Puka cheqche papalisa (PCP), Bela api chuqcha lisa (BACL), and Q'ello muro lisa (QML) varieties were conducted, with samples collected in 2024. Extraction yields ranged from 3.00 to 4.45%, viscosities from 6443.17 to 6892.77 cP, a high whiteness index from 90.43 to 93.52, water activity less than 0.55, and a heterogeneous particle size distribution. Amylose content ranged from 31.00 to 33.33%. FTIR analysis revealed similar functional groups and structural bonds across the varieties. For technofunctional properties, the QML variety exhibited greater water absorption, a higher solubility index, and greater swelling power. Pasting temperatures ranged from 68.70 to 71.10 °C, with low retrogradation. Thermal analysis showed good thermal stability from 104.46 to 268.42 °C, a low gelatinization temperature from 59.37 to 60.19 °C, and an enthalpy of up to 5.5757 J/g. Olluco starches have high potential for industrial applications, and their ease of cultivation makes them ideal for starch extraction.

Keywords: starch; olluco (*Ullucus tuberosus*); physical and chemical properties; technofunctional properties; thermal properties

Check for updates

Academic Editor: Lesław Juszczak

Received: 11 March 2026
Revised: 14 April 2026
Accepted: 2 May 2026
Published: 7 May 2026

Copyright: © 2026 by the authors. Licensee MDPI, Basel, Switzerland. This article is an open access article distributed under the terms and conditions of the Creative Commons Attribution (CC BY) license.

1. Introduction

The olluco (*Ullucus tuberosus*) is a tuber traditionally cultivated and consumed in high Andean regions such as Peru, Ecuador, and Bolivia [1,2]. This tuber can adapt to adverse climatic conditions and is also resistant to pests [1,3,4]. It is a food with high technological and nutritional value [5], and its significant starch content makes it a potential option for processing and industrialization [5,6]. Despite this, cultivation of this tuber has decreased considerably in recent years [7].

There are different varieties of olluco, among which the Puka cheqche papalisa (PCP), Bela api chuqcha lisa (BACL), and Q'ello muro lisa (QML) varieties are notable. These are cultivated and consumed in the province of Andahuaylas, Apurímac. Olluco is considered an underutilized food [1,8], with limited information available on the properties of its starches [9,10]. Therefore, it is necessary to investigate its physical, chemical, and technofunctional properties to support its use in industry.

Starches are the most abundant carbohydrates in nature and are found in large quantities in certain plant tissues such as tubers [11]. They are widely used in the food industry as thickeners, gelling agents, for pasta making, and as stabilizers [12]. Their widespread use makes them a high-demand product [13]. However, their application in the food industry presents limitations [14] because they exhibit physical, chemical, technofunctional, and thermal behaviors that depend on the extraction source [15,16]. Therefore, it is important to explore new extraction sources to industrialize them [17].

In Andean tubers, the physical, chemical, and technofunctional properties of starch depend on the amylose-to-amylopectin ratio [18]. Amylose, a linear polymer with α-1,4 linkages, produces firmer gels, greater retrogradation, and lower viscosity. Amylopectin, which is highly branched by α-1,4 and α-1,6 linkages, confers high viscosity, thermal stability, and less recrystallization. These differences determine the gelatinization, texture, and stability of the starches characteristic of Andean tubers [15,19].

The behavior of starch depends on its intrinsic properties and its response during processing [15]. For olluco, understanding these characteristics is essential to guide its technological applications. Higher amylose content produces firmer gels and films [18,20], while pasta production requires starches with good water absorption, solubility, and swelling power [21]. Applications such as gelling agents require high transparency and luminosity [22]; thickeners require high viscosity [15]; and bioplastics require low gelatinization temperature and high thermal stability [20,22]. Therefore, it is essential to explore alternative sources of olluco starch to enhance and optimize its industrial applications.

This study aimed to provide information on the physical, chemical, and technofunctional properties of starches extracted from three varieties of olluco by analyzing viscosity, color, water activity, thermal stability, density, particle size, amylose content, FTIR analysis, absorption index, solubility index, swelling power, paste clarity, pasting properties, and gelatinization temperature.

2. Materials and Methods

2.1. Raw Material

The collection of olluco tuber ecotypes included Bela api chuqcha lisa (BACL, elongated ellipsoid shape, 4–8 cm long and 2–4 cm wide, slightly rough surface, cream or pale yellow skin with pink spots, translucent cream pulp), Q'ello muro lisa (QML, oval, 3–6 cm long and 3–5 cm wide, intense yellow skin with small orange spots, cream to pale yellow pulp), and Puka cheqche papalisa (PCP, irregularly rounded, 3–6 cm in diameter, intense red or purple skin with yellow spots, white or pink pulp). The ecotypes were collected in April 2024, in the populated center of Rebelde Huayrana, located at 13°41′48.2″ S, 73°36′7.2″ W and 3339 m altitude, Santa María de Chicmo district, province of Andahuay-

las, Apurímac, Peru. The properties of the extracted starches are specific to the area, year, and growing conditions.

2.2. Starch Extraction

Ulluco tubers, free of bruises and blemishes, were washed with potable water and rinsed with distilled water. They were diced into 1 cm cubes and ground in a domestic blender (Oster Expert BLSTTDG-013, Boca Raton, FL, USA) with distilled water at a 1:2 ratio for 30 s. The mixture was then filtered through a sieve to separate the fibers and allowed to settle for 6 h at 4 °C. The sediment was washed by centrifugation (Pro Analytical CR4000R model, Centurion Scientific, West Sussex, UK) at 2236× *g* for 5 min. The wet starch (precipitate) was dried in an oven at 35 °C for 24 h. Finally, it was pulverized and stored in polyethylene containers at room temperature. Figure 1 shows the extraction sequence.

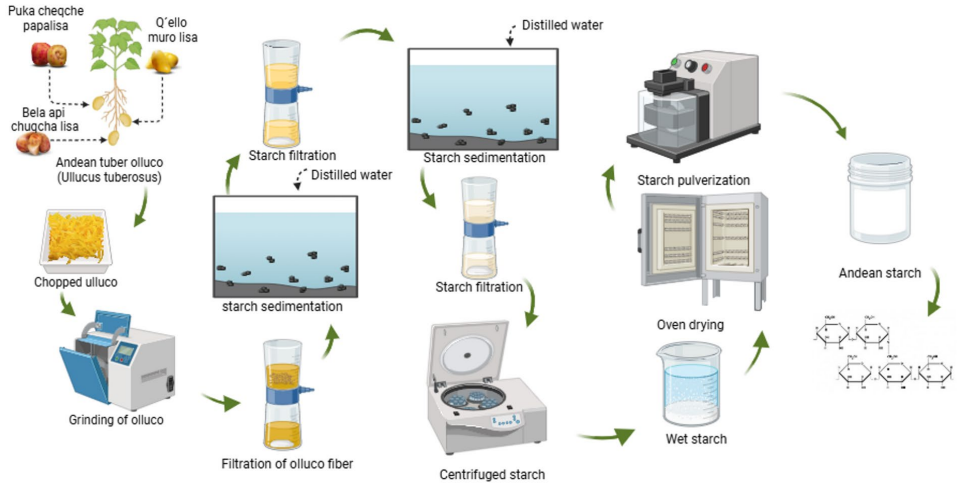


Figure 1. Wet extraction sequence of olluco starch.

2.3. Starch Extraction Yield

It was determined using Equation (1) [23]

$$Y\ (\%) = \frac{DWS}{WOT_t} \times 100 \quad (1)$$

where Y (%), extraction yield in percentage; DWS, dry weight of extracted starch; WOT, weight of whole olluco tubers.

2.4. Viscosity

The methodology proposed by Shi [24] was adapted. 25 g of dry starch were weighed and suspended in 500 mL of distilled water in a glass flask. The mixture was heated for 15 min at 80 °C with stirring and then allowed to cool to 25 °C. The viscosity was measured using a Fungilab PREMIUM series rotational viscometer (Barcelona, Spain) with spindle No. 3 at 10 rpm.

2.5. Starch Color

The color of the starch was determined using a Konica-Minolta CR-5 instrument (Tokyo, Japan) and the CIELab color space, where L* denotes lightness, a* indicates the color space with positive values tending toward red and negative values toward green, and b* tends toward yellow for positive values and blue for negative values. The white-

ness index (WI) and yellowness index (YI) were determined using Equations (2) and (3), respectively [18,25].

$$WI = 100 - \sqrt{(100 - L^*)^2 + (a^*)^2 + (b^*)^2} \quad (2)$$

$$YI = \frac{(142.86)(b^*)}{L^*} \quad (3)$$

2.6. Water Activity (a_w)

A portion of starch was placed on a plastic plate covering the surface, and the a_w was determined using Rotronic equipment, model Hygropalm23-AW (Bassersdorf, Switzerland).

2.7. Thermal Analysis

Ten milligrams of starch were weighed into aluminum crucibles and analyzed using a thermogravimetric analyzer (TGA 550, TA Instruments, New Castle, DE, USA). The analysis was conducted from 20 to 600 °C at a heating rate of 10 °C/min under a nitrogen flow of 50 mL/min. Before measurement, a baseline was established by passing nitrogen through the system [4].

The thermal transition of olluco starches was assessed using differential scanning calorimetry (DSC). Ten milligrams of starch were combined with deionized water in a 1:2 ratio to form a paste, which was placed in an aluminum tray and hermetically sealed. The sample was heated in a DSC instrument (DSC2500, TA Instruments, New Castle, DE, USA) from 20 to 120 °C at a rate of 5 °C/min under a nitrogen flow of 50 mL/min. TGA-DSC thermograms were analyzed with Trios V software (v5.8.1). A blank test using an empty crucible was performed beforehand to correct for baseline drift [4].

2.8. Functional Group Analysis

Functional groups were identified using Fourier transform infrared spectroscopy (FTIR). Homogenized starch samples (1%) were prepared as KBr pellets and analyzed using an FTIR spectrometer (Nicolet IS50, Thermo Fisher Scientific, Waltham, MA, USA). Spectra were recorded over the range of 400–4000 cm^{-1} at a resolution of 4 cm^{-1}. Before analysis, the instrument was calibrated using nitrogen gas to establish the baseline.

2.9. Amylose Determination

Amylose content was determined using a colorimetric method. Briefly, 10 mg of starch was mixed with 0.1 mL of 95% ethanol and 0.9 mL of 1 M sodium hydroxide. The mixture was allowed to stand at room temperature for 24 h to ensure complete solubilization. It was then diluted to 10 mL with ultrapure water, mixed thoroughly, and left to stand for 30 min.

Afterward, 0.5 mL of the solution was transferred, and 1 mL of 1 M glacial acetic acid was added, followed by 0.2 mL of Lugol's iodine solution. The mixture was diluted to 10 mL with ultrapure water and allowed to stand in the dark for 20 min for color development.

Finally, aliquots were transferred into microplate wells, and the amylose content was measured at 620 nm using a microplate reader (Synergy H1, BioTek Instruments, Inc., Winooski, VT, USA). Amylopectin content was calculated by difference, assuming that total starch consists of amylose and amylopectin (100%) [26].

2.10. Pasting Properties

Three grams of dry starch were dispersed in 30 mL of ultrapure water and analyzed using an Anton Paar RVA viscoamylograph (model MCR 702e, Graz, Austria). The standard thermal cycle included a pre-agitation step at 500 rpm for 1 min before measurement. The

temperature profile consisted of holding at 50 °C for 1 min, followed by heating to 95 °C and holding for 7 min, and finally cooling to 50 °C with a holding time of 2 min.

2.11. Particle Size Distribution

Five grams of starch was suspended in 50 mL of 99.5% isopropanol and sonicated for 60 s at 30% power. Particle size measurements were carried out using a dynamic light scattering (DLS) analyzer (Mastersizer 3000, Malvern Instruments, Worcestershire, UK) at a stirring speed of 1500 rpm, with a refractive index of 1.53.

The particle size distribution was expressed in terms of mean diameters $D_{[0.1]}$, $D_{[0.5]}$, and $D_{[0.9]}$, corresponding to the cumulative size distribution percentiles. Before measurement, a baseline was established using the instrument's autocorrelation function to ensure data accuracy.

2.12. Starch Shapes by Scanning Electron Microscopy

Starch samples were mounted on adhesive tape and sputter-coated with a gold–palladium layer. Imaging was performed at an accelerating voltage of 10 kV using a scanning electron microscope (JCM-7000 Plus, JEOL Ltd., Tokyo, Japan) [27].

2.13. Determination of the Water Absorption Index (WAI), Water Solubility Index (WSI), and Swelling Power (SP)

A 0.2 g of starch sample was dispersed in distilled water and adjusted to a final volume of 10 mL. The suspension was heated at 50, 60, 70, 80, and 90 °C for 30 min under continuous stirring. After heating, the samples were cooled to room temperature and centrifuged at 5000 rpm for 30 min.

The supernatant was carefully decanted, and the sediment (gel) was weighed. The supernatant was then dried in an oven at 90 °C for 24 h and weighed to determine the soluble fraction [28].

The WAI, WSI, and SP were determined using Equations (4)–(6).

$$WAI = \frac{gel\ weight\ (\mathrm{g})}{sample\ weight\ (\mathrm{g})} \tag{4}$$

$$WSI\ (\%) = \frac{supernatant\ dry\ weight\ (\mathrm{g})}{sample\ \ weight\ \ (\mathrm{g})} \times 100 \tag{5}$$

$$SP = \frac{gel\ weight\ \ (\mathrm{g})}{sample\ \ weight\ \ (\mathrm{g}) - supernatant\ dry\ weight\ (\mathrm{g})} \tag{6}$$

2.14. Paste Clarity and Bulk Density

To evaluate paste clarity, 1% starch was homogenized with distilled water and heated to complete gelatinization for 30 min under continuous stirring. After cooling to room temperature, light transmittance was measured at 650 nm under ambient conditions [11].

For bulk density, 10 g of starch was weighed and transferred into a 25 mL graduated cylinder. The cylinder was gently tapped to eliminate air spaces and ensure uniform packing. Bulk density was calculated as the ratio of sample mass to the volume occupied (g/mL) [11].

2.15. Statistical Analysis Techniques

All analyses were performed in triplicate, and the results are expressed as mean ± standard deviation. Statistical analysis was conducted using one-way analysis of variance (ANOVA). Differences among varieties were assessed using Tukey's multiple range test at a signif-

icance level of $p < 0.05$. Statistical analyses were performed using Microsoft Excel and OriginPro 2024b software.

3. Results and Discussions

3.1. Starches Yield

Figure 2 shows the starch yield of olluco, revealing a significant difference ($p < 0.05$) between varieties. The BACL variety reported the highest yield (4.45%, Table 1), whereas the PCP and QML varieties showed comparable values. Similar results have been reported in recent studies for the Bela api chuqcha lisa variety (approximately 4.63%) and the Q'ello muro lisa variety (approximately 3.60%) [29–31].

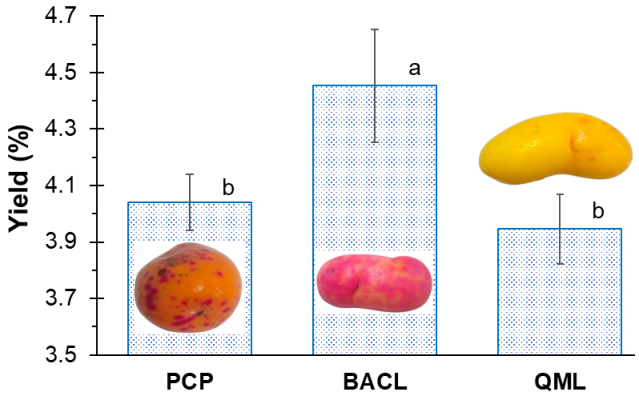


Figure 2. Olluco starch extraction yield. Different letters indicate significant differences evaluated through the Tukey test at 5% significance.

Table 1. Viscosity, color, and a_w values.

Parameters		PCP		BACL		QML	
		$\bar{x}$	±s	$\bar{x}$	±s	$\bar{x}$	±s
Yield (%)		4.04	0.10 b	4.45	0.20 a	3.95	0.12 b
Viscosity (cP)		6443.17	47.05 a	6590.63	80.85 a	6892.77	117.48 b
Color	L*	90.6	0.01 a	91.83	0.10 b	93.79	0.02 c
	a*	0.11	0.00 a	−0.1	0.01 b	−0.26	0.00 c
	b*	1.82	0.01 a	1.36	0.01 b	1.84	0.01 c
	WI	90.43	0.01 a	91.72	0.08 b	93.52	0.01 c
	YI	2.87	0.01 a	2.11	0.08 b	2.79	0.01 b
a_w		0.35	0.01 a	0.55	0.00 b	0.39	0.00 c

where $\bar{x}$ is the arithmetic mean, s is the standard deviation, a_w is water activity, WI is the white index, YI is the yellow index. Different letters indicate significant differences evaluated through the Tukey test at 5% significance.

Other tubers such as potato (*Solanum tuberosum* L.) and oca (*Oxalis tuberosa*) [18,32,33] generally present higher starch yields, whereas mashua (*Tropaeolum tuberosum*) exhibits lower values [16]. The observed variation in starch yield among the studied olluco varieties can be attributed to differences in botanical origin, genotype, management, and maturity [23,34].

3.2. Viscosity, Color, and Water Activity

The apparent viscosity of olluco starches showed significant differences ($p < 0.05$), with values ranging from 6443.17 to 6892.77 cP. The QML variety exhibited the highest viscosity (Table 1). These variations can be attributed to differences in starch composition and molecular structure among the evaluated varieties. In particular, phosphate group content

has been identified as a key factor influencing viscosity, as it promotes electrostatic repulsion between polymer chains and enhances granule swelling during gelatinization [35].

However, the fact that the BACL variety did not exhibit the highest viscosity suggests that additional structural factors—such as amylose content, granule thermal stability, and susceptibility to mechanical degradation during heating—also play a significant role in determining the rheological behavior of the paste. The results obtained are consistent with those reported by Valcárcel et al. [29] and Galíndez et al. [36], although they are higher than values reported in other studies [31,37].

These differences may be attributed to variations in experimental conditions, analytical techniques, and instrumentation, as well as intrinsic factors such as amylose content and shear rate, which influence the disruption of hydrogen bonding among amylose, amylopectin, and water [38,39].

Olluco starch exhibited a high whiteness index, associated with high lightness values (L > 90.60), as well as a low yellowness index, reflected in the reduced chromaticity values a* (−0.26 to 0.11) and b* (1.36 to 1.84) (Table 1). Significant differences ($p < 0.05$) were observed among the evaluated varieties. Comparable lightness results have been reported for olluco starch by Pico et al. [40]. These variations are mainly attributed to the botanical source, since the varieties of tubers differ in the content of anthocyanins, carotenoids, and other water-insoluble pigments [16,18,41].

Similarly, the double helix structure of amylopectin promotes the formation of complexes with proteins, lipids, and dietary fiber, which may lead to modifications in chromatic properties [18,42].

a_w is a key factor in food preservation, as it is directly related to degradation through biochemical reactions and the accelerated growth of microorganisms [43]. Therefore, maintaining low a_w levels is essential to ensure product stability and shelf life. Values ranging from 0.35 to 0.55 were observed in olluco starches (Table 1). These values are characteristic of tuber starches [4] and are considered low, indicating their resistance to microbial growth and chemical reactions [43].

Although a higher a_w value was observed for the BACL variety, this may be attributed to a greater content of free and bound water within the starch matrix, as well as a more amorphous structure that exposes hydroxyl groups, thereby promoting water adsorption and molecular mobility [44].

3.3. Amylose Content

The amylose and amylopectin content is a dominant factor in starch, as it has a major influence on its physical, chemical, techno-functional, and thermal properties [19]. It was observed that the starches of the three varieties studied ranged from 31.00 to 33.33% (p-value < 0.05), with greater content for QML (Table 2).

These differences may be attributed to the extraction technique, the method used for amylose determination, the botanical origin, genetic variability, soil conditions, and enzymatic activity during amylose biosynthesis. This activity contributes to the formation of structural voids within the starch granule following amylopectin synthesis [4,18,45].

Starch with a high amylose content is nutritionally beneficial, as it promotes slower starch digestibility. This property makes it particularly suitable for use in food products such as pasta, thickeners, gels, edible films, and pharmaceutical excipients [15,16,18,21,46], as well as for obtaining resistant starches and functional probiotic foods [32]. Although the amylose content in olluco varieties is lower than that in potatoes, it still exhibits desirable technofunctional properties, such as a relatively low gelatinization temperature.

Table 2. Amylose content in the starch of tuber varieties.

Starch Sources	Variety	Amylose %		Amylopectin %		Source
		$\bar{x}$	±s	$\bar{x}$	±s	
Olluco	PCP	31.33	0.58 b	68.67	0.58 a	In this study
	BACL	31.00	0.00 b	69	0.00 a	
	QML	33.33	1.53 a	66.67	1.53 b	
Native potato (*Solanum tuberosum* andigena)	AH	43.55	-	-	-	[4]
	AR	56.45	-	-	-	
Native potato	AP	38.92	-	-	-	[18]
	YKW	43.96	-	-	-	
	HM	36.29	-	-	-	
	YA	37.62	-	-	-	
Mashua (*Tropaeolum tuberosum*)	MNC	31.2	-	-	-	[16]
	MC	32.1	-	-	-	
Mashua	Blanca	28.23	-	-	-	[32]
	Amarilla	26.98	-	-	-	
Olluco	Roja	28.51	-	-	-	
	Amarilla	29.31	-	-	-	
Oca (*Oxalis tuberosa*)	Rosada	31.24	-	-	-	
Camote (*Oxalis tuberosa*)	Amarilla	33.68	-	-	-	
	Blanca	34.51	-	-	-	
Oca		27.6	-	-	-	[29]
Olluco		26.49	-	-	-	
Mashua		27.4	-	-	-	

where $\bar{x}$ is the arithmetic mean, and s is the standard deviation. The letters a and b indicate a significant difference evaluated through Tukey's test at a 5% significance level.

3.4. Thermal Stability Analysis

The TGA analysis showed three well-defined stages (Figure 3a). Total losses of 87.6, 88.84, and 92.68% were observed for BACL, PCP, and QML, respectively (Table 3). The first stage ends between 104.18 and 116.91 °C, with a mass loss of 11.26 to 12.77%, due to the removal of weakly bound water molecules and volatile components. Less weight loss is reported for PCP; this is due to its lower water content, which is related to its low aw (Table 1).

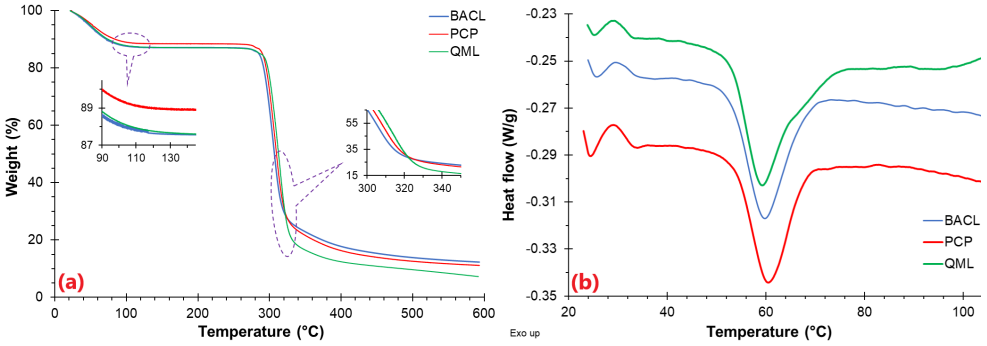


Figure 3. (**a**) TGA thermograms of olluco starches and (**b**) DSC thermograms of olluco starches.

Table 3. Weight loss in stages.

Variety	Stage 1					Stage 2						Stage 3						Residue (%)	Total Weight Loss (%)	
	T_i (°C)	T_f (°C)		Weight Loss		T_i (°C)		T_f (°C)		Weight Loss		T_i (°C)		T_f (°C)		Weight Loss				
		$\bar{x}$	±s	$\bar{x}$	±s	$\bar{x}$	±s	$\bar{x}$	±s	$\bar{x}$	±s	$\bar{x}$	±s	$\bar{x}$	±s	$\bar{x}$	±s		$\bar{x}$	±s
PCP	20	104.18	0.27	11.26	0.08 a	268.25	0.16	324.46	0.36	60.94	0.08 b	324.46	0.36	593.03	0.09	16.64	0.11 a	11.16	88.84	0.08 b
BACL	20	116.91	0.01	12.77	0.06 b	265.99	0.02	323.19	0.02	59.09	0.05 c	323.19	0.02	593.10	0.01	15.82	0.02 b	12.32	87.68	0.01 c
QML	20	116.06	0.22	12.69	0.05 b	252.31	0.45	333.19	0.41	67.66	0.03 a	333.19	0.41	593.09	0.09	12.33	0.11 c	7.32	92.68	0.13 a

Where T_i is the starting temperature, and T_f is the final temperature. Different letters indicate significant differences evaluated through the Tukey test at 5% significance.

The second stage, characterized by significant mass loss, begins between 252.31 and 268.25 °C and ends within the range of 323.19 to 333.19 °C. This stage is primarily associated with the depolymerization of starch chains [16,47], followed by the degradation of amylose and amylopectin mainly [48,49], lipid complexes and proteins [50,51]. During this process, volatile compounds such as bound water, carbon monoxide, carbon dioxide, acetaldehyde, furan, and 2-methylfuran are released [4,52,53], resulting in a weight loss ranging from 59.09 to 67.66% (Figure 3a and Table 3).

In the third stage, the final thermal degradation of olluco starch occurs, starting within the range of 323.19 to 333.19 °C and ending at 593.03 °C. This stage is associated with an additional weight loss of 12.33 to 16.64%, leaving a residual mass of 7.32 to 12.32%, which is attributed to the final decomposition of polysaccharides [50,51]. This process involves the formation of carbon dioxide from carbon monoxide, ultimately leaving carbonaceous material and mineral residues.

The higher residue content in BACL and PCP (Table 3) is likely due to the higher mineral content, which is related to the genotype and soil conditions of cultivation. Similarly, the lower residue reported by QML would indicate a higher carbohydrate content.

3.5. Thermal Behavior of Olluco Starches

The DSC analysis allowed us to determine the gelatinization temperature for PCP, BACL, and QML. This is represented by the area under the calorimetric peak, which includes the onset of gelatinization (T_0) (Figure 3b), due to water penetrating the starch granules and altering the hydrogen bonds in the amorphous regions of the structure, as well as the loss of crystalline regions, which causes structural changes.

Starch gelatinization depends on the molecular organization of amylopectin. T_0 for BACL starch was slightly lower (Table 4), suggesting the presence of less organized and less stable crystalline structures, which facilitates water penetration and the breaking of hydrogen bonds [32]. The T_p values showed no significant differences, indicating similar thermal stability of their crystalline structures with a similar energy distribution. However, this does not indicate the degree of crystallinity or amylose content, which is evaluated by comparing the gelatinization energy [4,54]. Conversely, the final temperature (T_f) was higher for QML and BACL (Table 4), indicating greater resistance to granule hydration, suggesting lower crystallinity due to amylose–amylose and amylose–amylopectin interactions.

Table 4. Temperature and enthalpy values for gelatinization of olluco starches.

Variety	T_o (°C)		T_p (°C)		T_f (°C)		ΔH	
	$\bar{x}$	±s	$\bar{x}$	±s	$\bar{x}$	±s	$\bar{x}$	±s
PCP	53.63	0.35 a	59.87	0.25 a	67.47	0.31 b	5.57	0.47 b
BACL	52.80	0.20 b	59.70	0.10 a	68.83	0.15 a	6.47	0.25 b
QML	53.03	0.40 a,b	60.00	0.20 a	68.37	0.15 a	7.47	0.35 a

Different letters indicate significant differences evaluated through the Tukey test at 5% significance.

High Andean tubers, such as potatoes, have similar T_0 values, while other tubers, such as mashua, have T_p values around 67.0 °C, and oca has lower T_f values [18,29,55]. The difference in T_p values between varieties and other tubers is attributed to the amylose–amylopectin ratio, chain length, granule size and shape, moisture content, and tuber maturity [29,56]. However, this low T_p causes olluco starches to have lower thermal stability and shear strength, as well as high retrogradation and resulting texture loss in high-temperature and high-maneuverability processes.

The ΔH values indicate higher gelation energy for the starches studied, in the order QML > BACL and PCP. This is related to the aw content, as more energy is needed to break the initial hydrogen bonds of water. Although the values found are lower than those for other starch sources, they enable gelatinization at lower temperatures. This reduces energy consumption, shortens processing time, and minimizes thermal damage to sensitive starch compounds. It also promotes the rapid formation of viscous pastes, which is ideal for instant foods. Thus, the gelatinization behavior of olluco starch depends on the crystalline structure of amylopectin, as shown by the T_p and ΔH values. While amylose mainly influences the T_f, allowing regulation of hydration behavior and complete granule disruption [56].

3.6. Functional Groups in Olluco Starches

Figure 4a shows the spectrum of the three olluco starch varieties. An intense peak was observed at 3265 cm^{-1}, corresponding to the stretching vibration of hydroxyl (-OH) groups of water and carbohydrates [32].

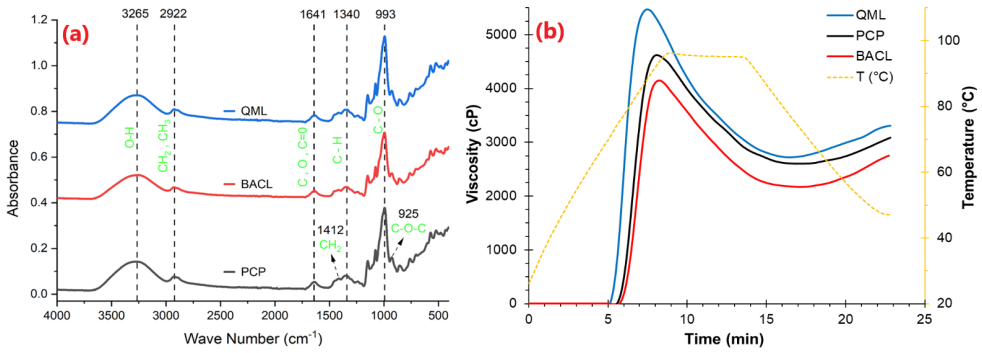


Figure 4. (**a**) FTIR spectrum of olluco starches and (**b**) RVA viscogram for olluco starches.

The peak at 2922 cm^{-1} is attributed to the stretching of C–H bonds (glucose anhydride), methylene groups (CH_2, CH_3) present in starch polysaccharides, and their rigid and amorphous regions in amylose and amylopectin [18,34]. Likewise, the peak at 1641 cm^{-1} is related to hydroxyl groups (-OH) bonded to water molecules, as well as to carbonyl groups (C=O) of the starch chain attached to the amide group [51,57], in addition to vibrations in the C-H and CH_2 bonds [58]. The peaks at 1412 and 1340 cm^{-1} were caused by the presence of water-soluble proteins [15].

At 993 cm^{-1}, a spectrum with high intensity is observed. This is attributed to vibrations in both the crystalline and amorphous regions of starch, as well as interactions between OH groups with the ester group of the glucose ring, C-O and C-C bonds in polysaccharide molecules, and glycosidic linkages in amylose and amylopectin [57,58]. This characteristic imparts unique structural properties to starches [19,49,57]. The intensity of this peak is associated with more rigid and ordered regions of the starch structure, suggesting that starches with a certain degree of crystallinity can be considered [11,32].

3.7. Pasting Behavior for Olluco Starches

The paste temperature marks the onset of viscosity increase as starch granules absorb water, reflecting their rupture and irreversible swelling. This shows that water becomes accessible to the amorphous regions of the granule, rather than indicating complete gelatinization [15,56,59]. The pasting temperatures of the varieties showed no significant differences, with values around 68.87 °C for QML, 70.63 °C for BACL, and 70.97 °C for PCP, which correspond to the results reported by the DSC analysis. Low gelatinization temperatures compared to other starch sources [18,29,55] indicate a granular structure with lower internal stability, allowing for easier hydration and swelling. Similarly, the short cooking time of approximately 4.86 min (Figure 5b) demonstrates a rapid state transition, which is ideal for industrial applications such as thickening agents, sterilizing agents, and baby foods, compared to other starch sources with slightly higher values [41].

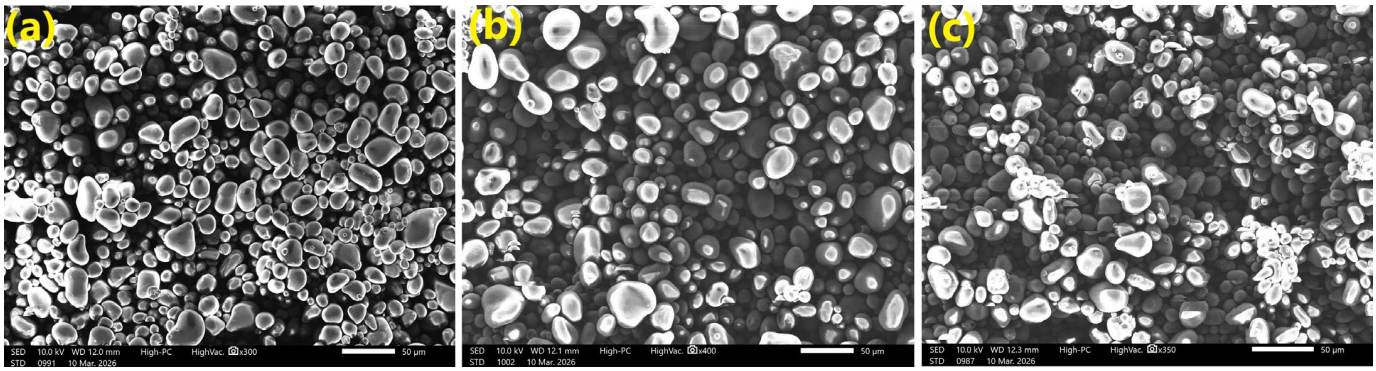


Figure 5. SEM images of starches (**a**) PCP, (**b**) BACL, (**c**) QML.

Amylopectin swelling is a key factor influencing the maximum viscosity of starches. During heating, it promotes granule expansion, leading to an increase in viscosity. Simultaneously, amylose acts as a limiting agent by restricting excessive swelling. In the RVA pasting profile, the BACL variety, after reaching its peak viscosity, exhibited a decline to 2159.26 cP (Figure 4b), indicating moderate resistance to mechanical shear and thermal stability [39]. This decrease may be associated with the disruption and collapse of swollen starch granules [21,41,60].

Following the decrease in viscosity, amylose molecules can reassociate during cooling through retrogradation. This process is reflected in an increase in final viscosity [39]. The QML starch exhibited a higher final viscosity (3322.04 cP) compared to PCP and BACL (Table 5), indicating a greater capacity for gel network formation and molecular reorganization. Rapid retrogradation is primarily associated with amylose, whereas slower retrogradation during storage is attributed to amylopectin [4].

Table 5. Pasting properties in starches of olluco varieties.

Parameters	PCP		BACL		QML	
	$\bar{x}$	±s	$\bar{x}$	±s	$\bar{x}$	±s
Pasting Temperature (°C)	70.97	0.67 a	70.63	1.34 a	68.87	0.57 a
Peak Viscosity (cP)	4621.16	24.76 b	4162.29	13.28 c	5507.37	18.14 a
Breakdown (cP)	2030.89	11.86 b	2003.03	10.88 c	2805.57	2.06 a
Holding Strength (cP)	2590.27	15.01 b	2159.26	10.25 c	2701.80	16.28 a
Setback From Peak (cP)	−1541.88	5.53 b	−1421.09	10.47 a	−2185.33	12.05 c
Setback From Trough (cP)	489.00	6.34 c	581.94	2.88 b	620.24	10.62 a
Final Viscosity (cP)	3079.28	19.76 b	2741.20	12.87 c	3322.04	7.76 a

Different letters indicate significant differences evaluated through the Tukey test at 5% significance.

Therefore, a higher final viscosity does not necessarily indicate lower retrogradation, but rather a stronger structural network formed after cooling. This behavior is desirable in applications such as baking and gel-based food systems [21,61].

3.8. Particle Size Distribution and Image of Starch Shapes

The particle size and starch shapes, in addition to depending on the source of traction, is crucial, as it defines the specific surface area and the amorphous and crystalline domains of the molecules, defining the mechanisms of hydration and molecular interaction, through hydrogen bonds, electrostatic attractions such as dipole–dipole, Van der Waals forces, and amylose–lipid–protein complexation. Fine granules (smaller than ($D_{[0.1]}$)) favor swelling, gelatinization, and increased apparent viscosity, while larger particles exhibit structural stability, affecting rheological behavior and techno-functional properties, which are crucial in the food, pharmaceutical, and cosmetic fields. It was observed that $D_{[0.1]}$ ranged from 11.88 to 13.76 µm, being lower for QML, exhibiting a relatively more spherical shape compared to the other starches (Figure 5c).

For $D_{[0.5]}$, values ranged from 24.71 to 36.30 µm, while for $D_{[0.9]}$, markedly different sizes were reported, with the largest being for BACL (Table 6). The larger average size of BACL (551.04 µm) is due to the formation of starch granule agglomerates through electrostatic interactions, with less defined and irregular shapes (Figure 5b), while PCP has a more elongated shape (Figure 5a). The differences in the shapes of the granules are due to the deposition, nucleation, and compaction of amylose and amylopectin in the available space of the amyloplast, manifesting isotropic or anisotropic growth, which gives rise to elongated, spherical, mixed and irregular shapes [6,16,30].

Table 6. Particle size distribution of olluco starch.

Variety	Granule Size (µm)								Transparency		Bulk Density (g/mL)	
	$D_{[0.1]}$		$D_{[0.5]}$		$D_{[0.9]}$		$Average_{[4.3]}$					
	$\bar{x}$	±s	$\bar{x}$	±s	$\bar{x}$	±s	$\bar{x}$	±s	$\bar{x}$	±s	$\bar{x}$	±s
PCP	11.94	0.81 b	25.88	3.07 b	305.06	21.81 c	87.75	5.92 c	7.96	2.66 a	0.82	0.01 a
BACL	13.76	0.81 a	36.30	1.98 a	1714.61	69.51 a	551.04	18.94 a	20.16	6.98 b	0.83	0.01 b
QML	11.88	0.43 b	24.71	1.18 b	520.09	22.53 b	139.30	7.84 b	18.89	0.63 b	0.8	0.01 a

where $\bar{x}$ is the arithmetic mean and *s* is the standard deviation. Different letters indicate significant differences evaluated through the Tukey test at 5% significance.

Therefore, the results indicated that the particle size distribution was not homogeneous, as different average granule sizes were obtained. However, this behavior has been observed in numerous studies for oca, olluco, and potato starches [16,18,37,45].

The difference in size compared to other tubers is attributed to biological origin and genotype, as well as to the amylopectin content in the granule, whose presence allows the formation of large granules [45,62,63], which is contrasted with the results reported in Table 2.

3.9. Transparency of the Paste and Density

Pasta clarity or transparency is an important technological property of starch, highly valued in the food industry, especially in products where transparency is key to the food's appearance. For example, high clarity is required in fruit coatings, while opaque starch is commonly used in the culinary industry [64]. Olluco starches exhibited a clarity of 7.96 to 20.16%, with the BACL variety showing the highest value (Table 6).

Although potato and mashua starches show improved transparency values [4,16], starches derived from quinoa and other cereals exhibit lower transparency. The trans-

parency of starch pastes depends largely on their high amylose content, as this promotes the absorption and swelling of the grain in suspension with water, hindering light transmission through the gel [11]. Furthermore, it has been noted that the increased clarity of starch paste is due to the phosphate-monoester derivative, while the presence of phospholipids and hydrophobic chromophores makes the paste opaque [65]. According to the results, BACL and QML could be used as coating or packaging materials for food and pharmaceuticals.

Furthermore, the bulk density of starches provides information on the distribution, packing, and compaction of granules during storage and handling [11]. They exhibited a density of 0.80 to 0.83 g/mL (p-value < 0.05) (Table 6). Density is related to granule size; therefore, BACL starch reported a slightly higher value.

3.10. Water Absorption Index (WAI), Water Solubility Index (WSI), and Swelling Power (SP) of Starches

When starches are heated in abundant water, their structure is modified, allowing the entry and association of water molecules through hydrogen bonds with the hydroxyl groups of amylose and amylopectin, causing absorption, solubility, and swelling [59].

The WAI shows an increasing behavior with respect to temperature (Figure 6a), with the greatest increase in the starch of the QML variety up to 27.98 g gel/g starch (Table 7), showing slightly significant differences with PCP and BACL. The difference could be due to the existence of molecularly rigid and amorphous regions at these temperatures, thus facilitating water penetration. Meanwhile, higher temperatures, lipid content, particle size and shape, and botanical source would contribute to water absorption in the core of the starch molecule [58]. Similarly, the weak structural formation after hydrolysis creates hydrophobic surfaces in small spaces of the internal walls of the structure, which generates the ease of water adsorption between varieties [66]. This depends on the type of starch and its conformation, with higher WSI values observed for other tubers such as potatoes [18,50,56].

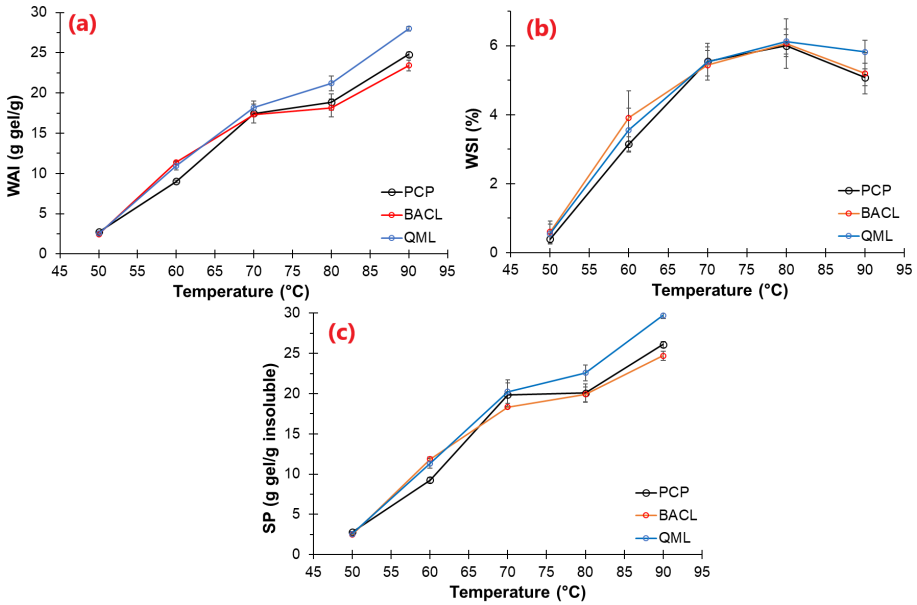


Figure 6. (**a**) Water absorption index, (**b**) water solubility index, and (**c**) swelling power.

Table 7. WAI, WSI, and SP values as a function of temperature.

Properties	Temperature (°C)	PCP		BACL		QML	
		$\bar{x}$	±s	$\bar{x}$	±s	$\bar{x}$	±s
WAI (g gel/g)	50	2.73	0.02 a	2.44	0.14 b	2.56	0.05 a,b
	60	9.00	0.18 b	11.39	0.20 a	10.95	0.49 a
	70	17.45	1.19 a	17.32	0.05 a	18.20	0.77 a
	80	18.86	1.00 a,b	18.16	1.10 b	21.19	0.92 a
	90	24.78	0.30 b	23.42	0.66 c	27.98	0.28 a
WSI (%)	50	0.39	0.06 b	0.60	0.05 a	0.55	0.03 a
	60	3.15	0.20 a	3.91	0.78 a	3.55	0.39 a
	70	5.55	0.42 a	5.43	0.43 a	5.53	0.53 a
	80	6.00	0.32 a	6.06	0.72 a	6.12	0.36 a
	90	5.08	0.24 a	5.20	0.60 a	5.82	0.33 a
SP (g gel/g insoluble)	50	2.79	0.08 a	2.46	0.14 b	2.57	0.06 a,b
	60	9.24	0.33 b	11.85	0.26 a	11.31	0.60 a
	70	19.85	0.60 a	18.31	0.11 a	20.25	1.46 a
	80	20.07	1.13 a,b	19.92	0.92 b	22.57	0.98 a
	90	26.11	0.38 b	24.70	0.57 c	29.70	0.36 a

Different letters indicate significant differences evaluated through the Tukey test at 5% significance.

The WSI of olluco starch showed no significant difference ($p < 0.05$), although it was significantly lower for PCP at 50 °C (Table 7), reaching its peak at 80 °C, similar for all varieties studied, decreasing slightly at 90 °C (Figure 6b). This could be attributed to reaching its maximum solubility limit, causing reorganization and interaction between amylose and amylopectin, forming insoluble complexes [58]. The slight difference at 90 °C between the varieties (5.82 for QML, 5.20 for BACL, and 5.08 for PCP) may be caused by the crystalline bonds between amylose and amylopectin, influencing the decrease in starch solubility [39], as well as by the phosphorus content, which is related to the solubility of starch in water [15,67].

On the other hand, amylose limits the SP of starch in water, as it can bind to lipid molecules, preventing interaction with water molecules [39,67,68]. Furthermore, it is associated with the rigid regions of amylopectin molecules [69,70] and even with the phosphorus molecules present in starch, which influence granule swelling [15,71,72]. The SP values obtained show an ascending curve as a function of temperature (Figure 6c), ranging from 2.57 to 29.70 g gel/g insoluble for QML, 2.46 to 24.70 g gel/g insoluble for BACL, and 2.79 to 26.11 g gel/g insoluble for PCP. Throughout the SP course, differences were observed between the starches (p-value < 0.05), being greater in most cases for QML.

3.11. Parameter Correlation Analysis

The correlational analysis reported that WAI, WSI, and SP showed a strong positive association with amylose content (Figure 7a). This is because linear chains are responsible for water penetration and the consequent partial disruption of the starch structure. Although these values correlated negatively with particle size and density, this suggests that olluco starch granules have compact and ordered structures, limiting water diffusion due to the stability of the crystalline regions formed by amylopectin. Therefore, the hydration of olluco starch depends on the molecular structure of the granule and, to a lesser extent, on the amylose content [49,73].

The transparency of the paste and WI were positively associated with WAI and WSI, indicating more homogeneous pastes with less light scattering due to high solubilization, while YI showed a negative relationship, probably associated with non-starch components.

This analysis suggests that optical properties could be considered indirect indicators of the degree of gelatinization and structural disorganization.

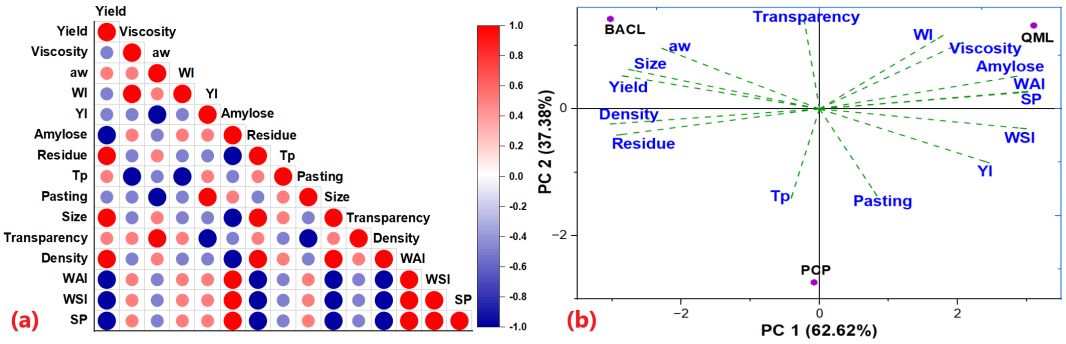


Figure 7. (**a**) Correlation of olluco starch parameters and (**b**) principal component analysis for olluco starch varieties.

Furthermore, principal component analysis (PCA), in which PC1 and PC2 explain 99.9% of the total variability (Figure 7b), reveals marked differences in the technofunctional behavior of the evaluated starch varieties. The QML variety is associated with higher values of WAI, SP, WSI, viscosity, amylose content, and whiteness index (WI), indicating a greater hydration capacity and enhanced technological performance.

In contrast, the BACL variety is characterized by larger particle size, higher yield, and increased a_w, suggesting a more compact structural organization. On the other hand, the PCP variety is associated with negative loadings on PC2, indicating a starch with improved gelling and paste-forming properties, which may confer greater thermal stability but reduced functionality in aqueous systems.

Thus, PCA demonstrated that the functional properties of the starches studied are not isolated; this behavior is attributed to the amylose-to-amylopectin ratio and particle size, which govern hydration, viscosity, and rheological behavior.

In this context, QML starch, exhibiting high hydration and viscosity, is a good candidate as a thickening agent and instant ingredient. On the other hand, BACL, which presents greater structural stability and less swelling, would be more appropriate for forming firm gels, coatings, biodegradable films, bioplastics, and as a polymeric agent, while PCP exhibits intermediate behavior.

4. Conclusions

Starch represents a strategic raw material for multiple industrial applications. Starches extracted in aqueous media from olluco tubers (PCP, BACL, and QML varieties) exhibited significant differences in their physicochemical and technofunctional properties, reflecting the strong influence of varietal origin on their structure and performance.

The starch from the QML variety showed a tendency toward a more organized functional structure, associated with higher viscosity, whiteness, and hydration capacity, as well as improved behavior in aqueous systems. These characteristics suggest a favorable profile for diverse industrial applications. In contrast, the BACL variety was characterized by greater structural and thermal stability. The PCP starch exhibited lower water activity and required less energy for gelatinization.

Pasting properties indicated rapid cooking behavior, high viscosity, and a low tendency toward retrogradation in all three varieties, demonstrating good stability upon cooling. These findings confirm the technological potential of olluco starch and highlight the importance of varietal differences as a key factor influencing its functionality and industrial applicability.

Further research focused on starch purification processes is recommended, as this remains a challenge and a promising area for future development.

Author Contributions: Conceptualization, D.C.-Q., E.S.O.P. and M.C.-F.; methodology, L.Q.C., Y.F.C.-M. and H.M.C.S.; validation, A.M.-Q., L.M.Z.-P. and J.W.E.-S.; formal analysis, D.C.-Q., E.S.O.P. and E.A.L.; investigation, E.S.O.P., Y.F.C.-M., M.C.-F., L.Q.C., H.M.C.S. and J.Q.C.; resources, D.C.-Q.; data curation, E.S.O.P.; writing—original draft preparation, D.C.-Q., E.S.O.P. and J.W.E.-S.; writing—review and editing, D.C.-Q., E.S.O.P. and C.A.B.C.; visualization, A.M.-Q., C.A.B.C. and D.C.-Q.; project administration, E.S.O.P.; funding acquisition, all authors. All authors have read and agreed to the published version of the manuscript.

Funding: This research received no external funding. The APC charges were covered by the authors.

Data Availability Statement: The original contributions presented in this study are included in the article. Further inquiries can be directed to the corresponding authors.

Acknowledgments: The authors would like to thank the Water Treatment Materials Research Laboratory (LIMTA), Agro-industrial research laboratory (LIA), Nanotechnology Research Laboratory (LINA), and the Vice-Rectorate for Research at the José María Arguedas National University, Andahuaylas, Perú. Likewise, to the rheology laboratory at the Universidad Nacional Intercultural de Quillabamba, Peru.

Conflicts of Interest: The authors declare that they have no conflicts of interest.

References

1. Flores-Marquez, R.; Vera-Vílchez, J.; Verástegui-Martínez, P.; Lastra, S.; Solórzano-Acosta, R. An evaluation of dryland ulluco cultivation yields in the face of climate change scenarios in the Central Andes of Peru by using the Aquacrop model. *Sustainability* **2024**, *16*, 5428. [CrossRef]
2. Condori, B.; Mamani, P.; Botello, R.; Patiño, F.; Devaux, A.; Ledent, J.F. Agrophysiological characterisation and parametrisation of Andean tubers: Potato (*Solanum* sp.), oca (*Oxalis tuberosa*), isaño (*Tropaeolum tuberosum*) and papalisa (*Ullucus tuberosus*). *Eur. J. Agron.* **2008**, *28*, 526–540. [CrossRef]
3. EFSA Panel on Plant Health (PLH); Bragard, C.; Dehnen-Schmutz, K.; Di Serio, F.; Gonthier, P.; Jacques, M.A.; Jaques Miret, J.A.; Justesen, A.F.; MacLeod, A.; Magnusson, C.S. Commodity risk assessment of *Ullucus tuberosus* tubers from Peru. *EFSA J.* **2021**, *19*, e06428. [CrossRef]
4. Choque-Quispe, D.; Gonzales, F.H.O.; Carranza-Oropeza, M.V.; Solano-Reynoso, A.M.; Ligarda-Samanez, C.A.; Palomino-Ríncón, W.; Choque-Quispe, K.; Torres-Calla, M.J. Physicochemical and technofunctional properties of high Andean native potato starch. *J. Agric. Food Res.* **2024**, *15*, 100955. [CrossRef]
5. Pérez, L.V.; Sánchez, H.J.; Cando, V.M.; Sánchez, Á.; Salazar, D.M. Fortification of low-fat yogurt with melloco flour (*Ullucus tuberosus*): Physicochemical and rheological effects. *Afr. J. Food Agric. Nutr. Dev.* **2022**, *22*, 22041–22058. [CrossRef]
6. Pacheco, M.T.; Moreno, F.J.; Moreno, R.; Villamiel, M.; Hernandez-Hernandez, O. Morphological, technological and nutritional properties of flours and starches from mashua (*Tropaeolum tuberosum*) and melloco (*Ullucus tuberosus*) cultivated in Ecuador. *Food Chem.* **2019**, *301*, 125268. [CrossRef] [PubMed]
7. Rodríguez, J.P.; Bonifacio, A.; Andrade, N.J.P.; Sørensen, M. Traditional uses, processes, and markets of ulluco (*Ullucus tuberosus* Caldas). In *Traditional Starch Food Products*; Elsevier: Amsterdam, The Netherlands, 2025; pp. 373–384.
8. Zambrano, J.L.A.; de Oliveira Paulino, F.; da Cruz, D.D. Roots and tubers in Colombia's culinary and food traditions. In *Traditional Starch Food Products*; Elsevier: Amsterdam, The Netherlands, 2025; pp. 113–127.
9. Salazar, D.; Arancibia, M.; Ocaña, I.; Rodríguez-Maecker, R.; Bedón, M.; López-Caballero, M.E.; Montero, M.P. Characterization and technological potential of underutilized ancestral andean crop flours from Ecuador. *Agronomy* **2021**, *11*, 1693. [CrossRef]
10. Cereda, M.P.; Vilpoux, O.F. Introduction: Importance of South American underground starchy crops. In *Starchy Crops Morphology, Extraction, Properties and Applications*; Elsevier: Amsterdam, The Netherlands, 2023; pp. 1–15.
11. Dubey, N.; Yadav, N.; Kaur, D. Physicochemical, Functional, and Structural Characterization of Quinoa (*Chenopodium quinoa*) Starch Modified by Heat Moisture Treatment, Annealing, and Gelatinization-Retrogradation. *Starch-Stärke* **2025**, *77*, e70080. [CrossRef]
12. Himashree, P.; Sengar, A.S.; Sunil, C.K. Food thickening agents: Sources, chemistry, properties and applications-A review. *Int. J. Gastron. Food Sci.* **2022**, *27*, 100468. [CrossRef]

13. Kumar, Y.; Shikha, D.; Guzmán-Ortiz, F.A.; Sharanagat, V.S.; Kumar, K.; Saxena, D.C. Starch: Current production and consumption trends. In *Starch: Advances in Modifications, Technologies and Applications*; Springer: Berlin/Heidelberg, Germany, 2023; pp. 1–10.
14. Zarski, A.; Bajer, K.; Kapuśniak, J. Review of the most important methods of improving the processing properties of starch toward non-food applications. *Polymers* **2021**, *13*, 832. [CrossRef]
15. Cornejo-Ramírez, Y.I.; Martínez-Cruz, O.; Del Toro-Sánchez, C.L.; Wong-Corral, F.J.; Borboa-Flores, J.; Cinco-Moroyoqui, F.J. The structural characteristics of starches and their functional properties. *CyTA-J. Food* **2018**, *16*, 1003–1017. [CrossRef]
16. Daza, L.D.; Umaña, M.; Simal, S.; Váquiro, H.A.; Eim, V.S. Non-conventional starch from cubio tuber (*Tropaeolum tuberosum*): Physicochemical, structural, morphological, thermal characterization and the evaluation of its potential as a packaging material. *Int. J. Biol. Macromol.* **2022**, *221*, 954–964. [CrossRef]
17. Huang, T.-T.; Zhou, D.-N.; Jin, Z.-Y.; Xu, X.-M.; Chen, H.-Q. Effect of debranching and heat-moisture treatments on structural characteristics and digestibility of sweet potato starch. *Food Chem.* **2015**, *187*, 218–224. [CrossRef]
18. Mojo-Quisani, A.; Licona-Pacco, K.; Choque-Quispe, D.; Calla-Florez, M.; Ligarda-Samanez, C.A.; Mamani-Condori, R.; Florez-Huaracha, K.; Huamaní-Melendez, V.J. Physicochemical properties of starch of four varieties of native potatoes. *Heliyon* **2024**, *10*, e35809. [CrossRef]
19. Velasquez Barreto, F.F.; Bello-Pérez, L.A. Chemical, structural, technological properties and applications of Andean tuber starches: A review. *Food Rev. Int.* **2023**, *39*, 1293–1308. [CrossRef]
20. Choque-Quispe, D.; Froehner, S.; Ligarda-Samanez, C.A.; Ramos-Pacheco, B.S.; Palomino-Rincón, H.; Choque-Quispe, Y.; Solano-Reynoso, A.M.; Taipe-Pardo, F.; Zamalloa-Puma, L.M.; Calla-Florez, M. Preparation and chemical and physical characteristics of an edible film based on native potato starch and nopal mucilage. *Polymers* **2021**, *13*, 3719. [CrossRef] [PubMed]
21. Wang, J.; Li, Y.; Guo, X.; Zhu, K.; Wu, Z. A review of the impact of starch on the quality of wheat-based noodles and pasta: From the view of starch structural and functional properties and interaction with gluten. *Foods* **2024**, *13*, 1507. [CrossRef]
22. Mojo-Quisani, A.; Ccallo-Silva, D.A.; Choque-Quispe, D.; Calla-Florez, M.; Ligarda-Samanez, C.A.; Comettant-Rabanal, R.; Mamani-Condori, R.; Huamaní-Meléndez, V.J. Development of edible films based on nostoc and modified native potato starch and their physical, mechanical, thermal, and microscopic characterization. *Polymers* **2024**, *16*, 2396. [CrossRef]
23. Jiang, Z.; Wei, Z.; Zhang, J.; Zheng, C.; Zhu, H.; Zhai, H.; He, S.; Gao, S.; Zhao, N.; Zhang, H. Source-sink synergy is the key unlocking sweet potato starch yield potential. *Nat. Commun.* **2024**, *15*, 7260. [CrossRef] [PubMed]
24. Shi, X.; BeMiller, J.N. Effects of food gums on viscosities of starch suspensions during pasting. *Carbohydr. Polym.* **2002**, *50*, 7–18. [CrossRef]
25. Hsu, C.-L.; Chen, W.; Weng, Y.-M.; Tseng, C.-Y. Chemical composition, physical properties, and antioxidant activities of yam flours as affected by different drying methods. *Food Chem.* **2003**, *83*, 85–92. [CrossRef]
26. McGrance, S.J.; Cornell, H.J.; Rix, C.J. A simple and rapid colorimetric method for the determination of amylose in starch products. *Starch-Stärke* **1998**, *50*, 158–163. [CrossRef]
27. Bekele, D.W.; Admassu, S. Pasting, thermal and structural properties of haricot beans flour (*Phaseolus vulgaris*, L.) as affected by variety and germination. *Int. J. Food Prop.* **2023**, *26*, 963–973. [CrossRef]
28. Anderson, R.A. Water absorption and solubility and amylograph characteristics of roll-cooked small grain products. *Cereal Chem.* **1982**, *59*, 265–269.
29. Valcárcel-Yamani, B.; Rondán-Sanabria, G.G.; Finardi-Filho, F. The physical, chemical and functional characterization of starches from Andean tubers: Oca (*Oxalis tuberosa* Molina), olluco (*Ullucus tuberosus* Caldas) and mashua (*Tropaeolum tuberosum* Ruiz & Pavón). *Braz. J. Pharm. Sci.* **2013**, *49*, 453–464. [CrossRef]
30. Torres, F.G.; Troncoso, O.P.; Díaz, D.A.; Amaya, E. Morphological and thermal characterization of native starches from Andean crops. *Starch-Stärke* **2011**, *63*, 381–389. [CrossRef]
31. Velásquez-Barreto, F.F.; Bello-Pérez, L.A.; Nuñez-Santiago, C.; Yee-Madeira, H.; Sanchez, C.E.V. Relationships among molecular, physicochemical and digestibility characteristics of Andean tuber starches. *Int. J. Biol. Macromol.* **2021**, *182*, 472–481. [CrossRef]
32. Fonseca-Santanilla, E.B.; Betancourt-López, L.L. Physicochemical and structural characterization of starches from Andean roots and tubers grown in Colombia. *Food Sci. Technol. Int.* **2022**, *28*, 144–156. [CrossRef] [PubMed]
33. Zhao, X.; Hofvander, P.; Andersson, M.; Andersson, R. Internal structure and thermal properties of potato starches varying widely in amylose content. *Food Hydrocoll.* **2023**, *135*, 108148. [CrossRef]
34. Nawaz, A.; Ali, S.W.; Irshad, S.; Irshad, F.; Ahmed, A.; Sharmeen, Z.; Khan, I. Effect of peeling and unpeeling on yield, chemical structure, morphology and pasting properties of starch extracted from three diverse potato cultivars of Pakistan. *Int. J. Food Sci. Technol.* **2020**, *55*, 2344–2351. [CrossRef]
35. Zhu, F.; Cui, R. Comparison of physicochemical properties of oca (*Oxalis tuberosa*), potato, and maize starches. *Int. J. Biol. Macromol.* **2020**, *148*, 601–607. [CrossRef] [PubMed]
36. Galindez, A.; Daza, L.D.; Homez-Jara, A.; Eim, V.S.; Váquiro, H.A. Characterization of ulluco starch and its potential for use in edible films prepared at low drying temperature. *Carbohydr. Polym.* **2019**, *215*, 143–150. [CrossRef]

37. Velásquez-Barreto, F.F.; Bello-Pérez, L.A.; Yee-Madeira, H.; Velezmoro Sánchez, C.E. Esterification and characterization of starch from Andean tubers. *Starch-Stärke* **2019**, *71*, 1800101. [CrossRef]
38. Guo, K.; Lin, L.; Fan, X.; Zhang, L.; Wei, C. Comparison of structural and functional properties of starches from five fruit kernels. *Food Chem.* **2018**, *257*, 75–82. [CrossRef]
39. Guo, K.; Tian, Y.; Podzimska-Sroka, D.; Kirkensgaard, J.J.K.; Herburger, K.; Enemark-Rasmussen, K.; Hassenkam, T.; Petersen, B.L.; Blennow, A.; Zhong, Y. Structural evolution of maize starches with different amylose content during pasting and gelation as evidenced by rapid Visco Analyser. *Food Chem.* **2024**, *461*, 140817. [CrossRef] [PubMed]
40. Pico, C.; De la Vega, J.; Tubón, I.; Arancibia, M.; Casado, S. Nanoscopic Characterization of Starch Biofilms Extracted from the Andean Tubers *Ullucus tuberosus*, *Tropaeolum tuberosum*, *Oxalis tuberosa*, and *Solanum tuberosum*. *Polymers* **2022**, *14*, 4116. [CrossRef]
41. Wang, H.; Yang, Q.; Gao, L.; Gong, X.; Qu, Y.; Feng, B. Functional and physicochemical properties of flours and starches from different tuber crops. *Int. J. Biol. Macromol.* **2020**, *148*, 324–332. [CrossRef]
42. Feng, T.; Zhuang, H.; Chen, F.; Campanella, O.; Bhopatkar, D.; Carignano, M.A.; Park, S.H. Starch-lipid and starch-protein complexes and their application. In *Functional Starch and Applications in Food*; Springer: Berlin/Heidelberg, Germany, 2018; pp. 177–226.
43. Ocieczek, A.; Mesinger, D.; Toczek, H. Hygroscopic properties of three cassava (Manihot esculenta Crantz) starch products: Application of BET and GAB models. *Foods* **2022**, *11*, 1966. [CrossRef]
44. Hoover, R. Composition, molecular structure, and physicochemical properties of tuber and root starches: A review. *Carbohydr. Polym.* **2001**, *45*, 253–267. [CrossRef]
45. Barraza-Jáuregui, G.; Soriano-Colchado, J.; Obregón, J.; Martínez, P.; Peña, F.; Velezmoro, C.; Siche, R.; Miano, A.C. Physicochemical, functional and structural properties of starches obtained from five varieties of native potatoes (*Solanum tuberosum* L.). In Proceedings of the 18th LACCEI International Multi-Conference for Engineering, Education, and Technology: "Engineering, Integration, and Alliances for a Sustainable Development" "Hemispheric Cooperation for Competitiveness and Prosperity on a Knowledge-Based Economy", Online, 27–31 July 2020; pp. 1–10.
46. Choque-Quispe, D.; Froehner, S.; Palomino-Rincón, H.; Peralta-Guevara, D.E.; Barboza-Palomino, G.I.; Kari-Ferro, A.; Zamalloa-Puma, L.M.; Mojo-Quisani, A.; Barboza-Palomino, E.E.; Zamalloa-Puma, M.M. Proposal of a water-quality index for high Andean basins: Application to the Chumbao river, Andahuaylas, Peru. *Water* **2022**, *14*, 654. [CrossRef]
47. Liu, Y.; Yang, L.; Ma, C.; Zhang, Y. Thermal behavior of sweet potato starch by non-isothermal thermogravimetric analysis. *Materials* **2019**, *12*, 699. [CrossRef] [PubMed]
48. Martins, A.; Beninca, C.; Bet, C.D.; Bisinella, R.Z.B.; de Oliveira, C.S.; Hornung, P.S.; Schnitzler, E. Ultrasonic modification of purple taro starch (*Colocasia esculenta* B. Tini): Structural, psychochemical and thermal properties. *J. Therm. Anal. Calorim.* **2020**, *142*, 819–828. [CrossRef]
49. Zhao, T.; Zhang, H.; Chen, F.; Tong, P.; Cao, W.; Jiang, Y. Study on structural changes of starches with different amylose content during gelatinization process. *Starch-Stärke* **2022**, *74*, 2100269. [CrossRef]
50. Thakur, M.; Rai, A.K.; Singh, S.P. Structural characteristics, physicochemical properties, and digestibility analysis of resistant starch type-V prepared from debranched corn starch and fatty acid complexation. *ACS Omega* **2023**, *8*, 25799–25807. [CrossRef]
51. Rodrigues, S.C.S.; da Silva, A.S.; de Carvalho, L.H.; Alves, T.S.; Barbosa, R. Morphological, structural, thermal properties of a native starch obtained from babassu mesocarp for food packaging application. *J. Mater. Res. Technol.* **2020**, *9*, 15670–15678. [CrossRef]
52. Liu, X.; Wang, Y.; Yu, L.; Tong, Z.; Chen, L.; Liu, H.; Li, X. Thermal degradation and stability of starch under different processing conditions. *Starch-Stärke* **2013**, *65*, 48–60. [CrossRef]
53. Bajer, D. Nano-starch for food applications obtained by hydrolysis and ultrasonication methods. *Food Chem.* **2023**, *402*, 134489. [CrossRef]
54. Ee, K.Y.; Eng, M.K.; Lee, M.L. Physicochemical, thermal and rheological properties of commercial wheat flours and corresponding starches. *Food Sci. Technol.* **2020**, *40*, 51–59. [CrossRef]
55. Colonna, P.; Buleon, A. Thermal transitions of starches. In *Starches: Characterization, Properties, and Applications*; CRC Press: Boca Raton, FL, USA, 2010; pp. 59–102.
56. Nogueira, G.F.; Carvalho, C.W.P.d.; Velasco, J.I.; Matta Fakhouri, F. Extraction and Characterization of Starches from Non-Conventional Sources: Turmeric (*Curcuma longa*) and Mangarito (*Xanthosoma sagittifolium*). *Polymers* **2025**, *17*, 3157. [CrossRef] [PubMed]
57. Hong, T.; Yin, J.-Y.; Nie, S.-P.; Xie, M.-Y. Applications of infrared spectroscopy in polysaccharide structural analysis: Progress, challenge and perspective. *Food Chem. X* **2021**, *12*, 100168. [CrossRef] [PubMed]
58. Montoya-Anaya, D.G.; Madera-Santana, T.J.; Aguirre-Mancilla, C.L.; Grijalva-Verdugo, C.; Gonzales-Garcia, G.; Nuñez-Colín, C.A.; Rodriguez-Nuñez, J.R. Physicochemical characterization of residual potato (*Solanum tuberosum*) starch recovered from the potato chips industry in Mexico. *Biotecnia* **2023**, *25*, 60–72.

59. Balet, S.; Guelpa, A.; Fox, G.; Manley, M. Rapid Visco Analyser (RVA) as a tool for measuring starch-related physiochemical properties in cereals: A review. *Food Anal. Methods* **2019**, *12*, 2344–2360. [CrossRef]
60. Tian, Y.; Qu, J.; Zhou, Q.; Ding, L.; Cui, Y.; Blennow, A.; Zhong, Y.; Liu, X. High pressure/temperature pasting and gelling of starch related to multilevel structure-analyzed with RVA 4800. *Carbohydr. Polym.* **2022**, *295*, 119858. [CrossRef]
61. Hu, H.; Lin, Q.; McClements, D.J.; Ji, H.; Jin, Z.; Qiu, C. Recent advances in the application of starch derivatives in baked foods: Effects on quality and functionality. *Trends Food Sci. Technol.* **2024**, *151*, 104647. [CrossRef]
62. Ratnaningsih, N.; Arovah, N.I. Structural, physicochemical properties, and resistant starch content of autoclaved arenga starch (*Arenga pinnata* (Wurmb) Merr). *Food Chem. Adv.* **2025**, *8*, 101090. [CrossRef]
63. Papilaya, E.; Akbar, M.; Togibasa, O. The Physico-chemical Characterisation of Sago Starch from Jayapura Regency. *Trends Carbohydr. Res.* **2022**, *14*, 71–80.
64. Valdés, A.; Martínez, C.; Garrigos, M.C.; Jimenez, A. Multilayer Films Based on Poly(lactic acid)/Gelatin Supplemented with Cellulose Nanocrystals and Antioxidant Extract from Almond Shell By-Product and Its Application on Hass Avocado Preservation. *Polymers* **2021**, *13*, 3615. [CrossRef] [PubMed]
65. Rosicka-Kaczmarek, J.; Kwaśniewska-Karolak, I.; Nebesny, E.; Komisarczyk, A. The functionality of wheat starch. In *Starch in Food*; Elsevier: Amsterdam, The Netherlands, 2018; pp. 325–352.
66. Jiang, K.; Wang, W.; Ma, Q.; Wang, J.; Sun, J. Microwave-assisted enzymatic hydrolysis as a novel efficient way to prepare porous starch. *Carbohydr. Polym.* **2023**, *301*, 120306. [CrossRef]
67. Vamadevan, V.; Bertoft, E. Observations on the impact of amylopectin and amylose structure on the swelling of starch granules. *Food Hydrocoll.* **2020**, *103*, 105663. [CrossRef]
68. Nuwamanya, E.; Baguma, Y.; Wembabazi, E.; Rubaihayo, P. A comparative study of the physicochemical properties of starches from root, tuber and cereal crops. *Afr. J. Biotechnol.* **2011**, *10*, 12018–12030.
69. Reddy, C.K.; Pramila, S.; Haripriya, S. Pasting, textural and thermal properties of resistant starch prepared from potato (*Solanum tuberosum*) starch using pullulanase enzyme. *J. Food Sci. Technol.* **2015**, *52*, 1594–1601. [CrossRef] [PubMed]
70. Vamadevan, V.; Bertoft, E. Impact of different structural types of amylopectin on retrogradation. *Food Hydrocoll.* **2018**, *80*, 88–96. [CrossRef]
71. Kaur, M.; Oberoi, D.P.S.; Sogi, D.S.; Gill, B.S. Physicochemical, morphological and pasting properties of acid treated starches from different botanical sources. *J. Food Sci. Technol.* **2011**, *48*, 460–465. [CrossRef] [PubMed]
72. Tester, R.F.; Morrison, W.R. Swelling and gelatinization of cereal starches. I. Effects of amylopectin, amylose, and lipids. *Cereal Chem.* **1990**, *67*, 551–557.
73. Reyniers, S.; De Brier, N.; Ooms, N.; Matthijs, S.; Piovesan, A.; Verboven, P.; Brijs, K.; Gilbert, R.G.; Delcour, J.A. Amylose molecular fine structure dictates water–oil dynamics during deep-frying and the caloric density of potato crisps. *Nat. Food* **2020**, *1*, 736–745. [CrossRef]

Disclaimer/Publisher's Note: The statements, opinions and data contained in all publications are solely those of the individual author(s) and contributor(s) and not of MDPI and/or the editor(s). MDPI and/or the editor(s) disclaim responsibility for any injury to people or property resulting from any ideas, methods, instructions or products referred to in the content.